Substrate thickness variation on the frequency response of microstrip antenna for mm-wave application

Bello Abdullahi Muhammad[1], Mohd Fadzil Ain[1], Mohd Nazri Mahmud[1], Mohd Zamir Pakhuruddin[2], Ahmadu Girgiri[1], Mohamad Faiz Mahamed Omar[3]

[1]School of Electrical and Electronic Engineering, Faculty of Engineering, Universiti Sains Malaysia, Pulau Pinang, Malaysia
[2]School of Physic, Faculty of Pure Science, Universiti Sains Malaysia, Pulau Pinang, Malaysia
[3]Collaborative Microelectronic Design Excellence Center (CEDEC), Pulau Pinang, Malaysia

Article Info

ABSTRACT

Substrate height (Hs) is an important parameter that influences antenna propagation. This research designed a low-profile 28 GHz microstrip antenna on a polyimide substrate with varying Hs using CST Studio software. The simulated results and MINITAB software were used to develop regression model equations, which analyzed the impact of Hs variation on the antenna performance. The proposed models' equations have indicated an increase in average responses of resonant frequency (Fr), percentage bandwidth (% BW), gain (G), return loss (RL), and efficiency (η) as the Hs decreased. The antenna achieved a BW of 3.87 GHz at Hs 0.525 mm and 5.54 GHz at 0.025 mm, a G of 3.89 dBi at Hs 0.525 mm and 3.91 dBi at Hs 0.025 mm, and an η of 94.19% at Hs 0.525 mm and 98.24% at Hs 0.025 mm. The antenna was fabricated and tested, and the experimental results were validated with the models' equations. The thinner substrate resulted in an improvement in the antenna performance.

Corresponding Author:

Mohd Fadzil Ain
School of Electrical and Electronic Engineering, Universiti Sains Malaysia Engineering Campus
14300 Nibong Tebal, Pulau Pinang, Malaysia
Email: eemfadzil@usm.my

1. INTRODUCTION

In recent years, wireless devices have become portable and require small antennas. Thus, substrate height (Hs) significantly impacts antenna portability and performance, as thinner substrate antennas are lightweight and portable [1]. The Hs employed propagation characteristics, such as electromagnetic field distribution with radiation efficiencies and resonating frequencies [2]. The relationship between the Hs variation and microstrip antenna performance is such that lower Hs generally perform better at high frequencies [3]. The lower Hs is applicable in higher-frequency applications, including a millimeter-wave (mm-wave) in the internet of things (IoT) and wearable devices [4]. Various substrates, including polyesters, textiles, and polymers with varying thicknesses and electrical properties, have been used in the antenna design [5].

However, the major challenge of designing a printable microstrip antenna is finding a suitable substrate and thickness with suitable dielectric constants. Changing the Hs affects the capacitance, effective dielectric constant, and inductive properties, causing a shift in the resonant frequency [6]. A substrate with a lower dielectric constant (ε_r=2.2, 3, or 4) achieved a wider bandwidth of the operating mm-wave frequency with a high gain, while a high dielectric constant of ε_r=10.2 leads to an increase in surface wave loss and dielectric loss [7]. A polymer-based substrate such as polyimide (PI) has been considered for low-profile antennas due to its lightweight and better performance [8]. PI has a low dielectric permittivity with a reduced dielectric constant to improve circuit integration [9]. A printable antenna using a thin Hs exhibits a broad

frequency range and high performance [10]. A thin substrate has been reported to improve antenna bandwidth and efficiency at high frequencies due to its dielectric permittivity [11].

A study investigates the design of antennas by stacking four different types of substrates to improve the antenna performance, in which thinner substrates lead to better performance [12]. An antenna array with a thin-film substrate significantly enhanced gain with a compact size [13]. The PI thin substrate is low-cost compared to thicker substrates in producing a low-cost antenna [14]. A fabricated microstrip antenna on a thin PI substrate decreased antenna weight by up to 92% compared to a thicker substrate antenna [15]. A thin PI substrate improved antenna bandwidth for wideband applications [16]. A PI substrate with varying thicknesses is proposed in this research work due to its flexibility, lightweight, and low power consumption. This article applied regression modeling to investigate the effect of Hs variation on the antenna performance using the regression models and the models' equations.

Different regression models include nonlinear, linear, multiple linear, and polynomial regression models. The model design depends on the dependent and independent variables (x and y). The x variable predicts the response of y. Several recent studies [17]–[20] illustrated the regression in (1)-(15) with the various methods. This article worked on polynomial regression and developed the proposed regression models that analyzed the relationship between dependent and independent variables.

$$Y \approx \beta_0 + \beta_1 X \tag{1}$$

$$y = \beta_0 + \beta_1 x + \in \tag{2}$$

$$y = \beta_0 + \beta_1 x + \cdots + \beta_n x + \in \tag{3}$$

$$y = \beta_0 + \beta_1 x^2 + \cdots + \beta_n x^n + \in \tag{4}$$

The y is the dependent variable, x is the independent variable, and x predicts the y response. β_0 is the y-intercept, and β_1 is the regression coefficient on the vertical axis of the regression line, which is the slope of the regression line. ε represented the random error and expressed the random factors' effect on the dependent variable. $\approx$ represents approximately, and (4) represents the polynomial equation.

$$\hat{y} = \hat{\beta}_0 + \hat{\beta}_1 X + \varepsilon \tag{5}$$

$$\hat{\beta}_1 = \frac{\sum_{i=1}^{n}(x_i - \bar{x})(y_i - \bar{y})}{\sum_i^n (x_{i=1}(x_i - \bar{x})^2)} \tag{6}$$

$$\hat{\beta}_0 = \bar{y} - \hat{\beta}_1 \bar{x} \tag{7}$$

$$\varepsilon = \tilde{X}\tilde{\beta} - y \tag{8}$$

$\hat{y}$ represents a prediction of Y where X represents x and the hat symbol denotes the estimated value for unknown parameters or coefficients in the predicted value of the response. The regression techniques will evaluate β_0 and β_1 and observe the sample (x_i, y_i) to the model parameters and the scatter diagram. The determination coefficients (Coef) are in (9) and (10).

$$RSS = \sum_{i-1}^{n}(y_i - \hat{y})^2 \tag{9}$$

$$RSE = \sqrt{\frac{1}{n-2}RSS} \tag{10}$$

RSS is a regression sum of squares, and RSE measures fitness, indicating whether the model fits or does not fit the data. The predicted value $\hat{y}$ is the original value of y. The Coef determined R-Square (R-Sq) analyzes the regression data of model performance and the strength of the relationship between the model and the data. The range of R-Sq is between 0 and 1. The higher value of R-Sq indicates the model to be optimal.

$$R - Sq = 1 - \frac{SS_{Error}}{SS_{Total}} \tag{11}$$

$$SS_{Error} = \sum_i (t_i - y_i)^2 \tag{12}$$

$$SS_{Total} = \sum_i (t_i - \bar{t}_i)^2 \tag{13}$$

SS_{Error} is the sum of the residual squares from the model, and SS_{Total} is the sum of squares of errors of the actual output and the mean of the output.

Since $R\text{-}Sq$ determines the fitness of data on the regression model, the model performance, the adjusted $R\text{-}Sq$ or modified $R\text{-}Sq$, is called $R\text{-}Sq$ adjust, which increases with the increased model performance. When unimportant features are added to the model and the residual error is reduced, the R-square adjustment ($R\text{-}Sq(adj)$) will also be reduced, and the R-Sq will increase.

$$R - Sq(adj) = 1 - \frac{(1-R-Sq)(N_v-1)}{N_v-N-1} \tag{14}$$

$$r = \sqrt{(R-Sq)}\text{r} \tag{15}$$

where N_V represents the number of the data sample, N is the number of features, making the $R\text{-}Sq(adj)$ more robust to the change of features, and r is the model correlation.

This article aims to address the issues of drawbacks in the 28 GHz printable microstrip antenna's parameters performance, such as resonant frequency (F_r), bandwidth (BW), gain (G), and efficiency (η) caused by the variation of Hs. To investigate, analyze, evaluate, and validate the experimental results and the regression models' equations. The proposed model and mathematical model equations were used to give insight to the antenna designers on how to enhance the antenna's parameters and the overall antenna's performance.

2. METHOD
2.1. Antenna design and configuration

The antenna design and configuration used a coplanar waveguide (CPW) with two slots on the patch and a gap between the feedline and the patch, as illustrated in Figure 1. The substrate thickness was varied to analyze the impact of PI substrate thicknesses (Hs) on the antenna's performance. Understanding the dielectric material is necessary since the dielectric material has a significant role in the antenna performance. The proposed antenna has a dielectric constant of ε_r=3.5 and a loss tangent, δ=0.0027, designed with various substrate thicknesses. The variation of Hs has a significant impact on the antenna's performance. The slotted CPW printable antenna with a compact size of 5×5×0.125 mm³ was designed and fabricated. The antenna has a bidirectional radiation pattern suitable for IoT and biomedical applications. It has a bandwidth of (26.200 GHz - 30.242 GHz) with a return loss (RL) of 22.62 dB and achieved a gain of 3.81 dBi and 96.21% efficiency. Table 1 shows the proposed antenna dimensions, and Figure 1 shows the proposed antenna design. The impact of Hs variation on these parameters was investigated, analyzed, evaluated, and validated by the simulated and measured results and regression modeling.
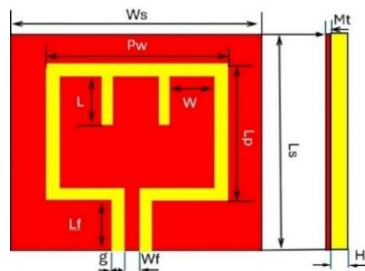

Figure 1. Proposed 28 GHz microstrip antenna

Table 1. Antenna dimensions

Parameter	Ls	Ws	Mt	Hs	Lf	Wp	Lp	Wf	g	L	W
Dimension (mm)	5	5	0.035	0.125	2.15	3.1	1.95	0.4	0.15	1.00	0.95

3. RESULTS AND DISCUSSION
3.1. Simulated result and discussion

The simulated results in Figures 2(a) to (d) illustrate the effect of varying Hs on the frequency response characteristics. The Figure 2 show the simulated result with various Hs values ranging from (a) 0.025 mm to 0.075 mm, (b) 0.100 mm to 0.150 mm, (c) 0.175 mm to 0.225 mm, and (d) 0.250 mm to 0.300 mm at which the frequencies resonated. The results demonstrated how Hs variation causes a shift in center frequency, BW and RL.

Generally, the results in Table 2 show that the lower the Hs, the higher the η, while the higher the Hs, the lower the η. And the thicker the substrate, the higher the BW and G, but a thinner substrate of 0.025 mm to 0.125 mm leads to good impedance matching. These resulted in an improvement in the BW and G from 3.6 GHz to 5.54 GHz and from 3.8 dBi to 3.91 dBi, respectively.
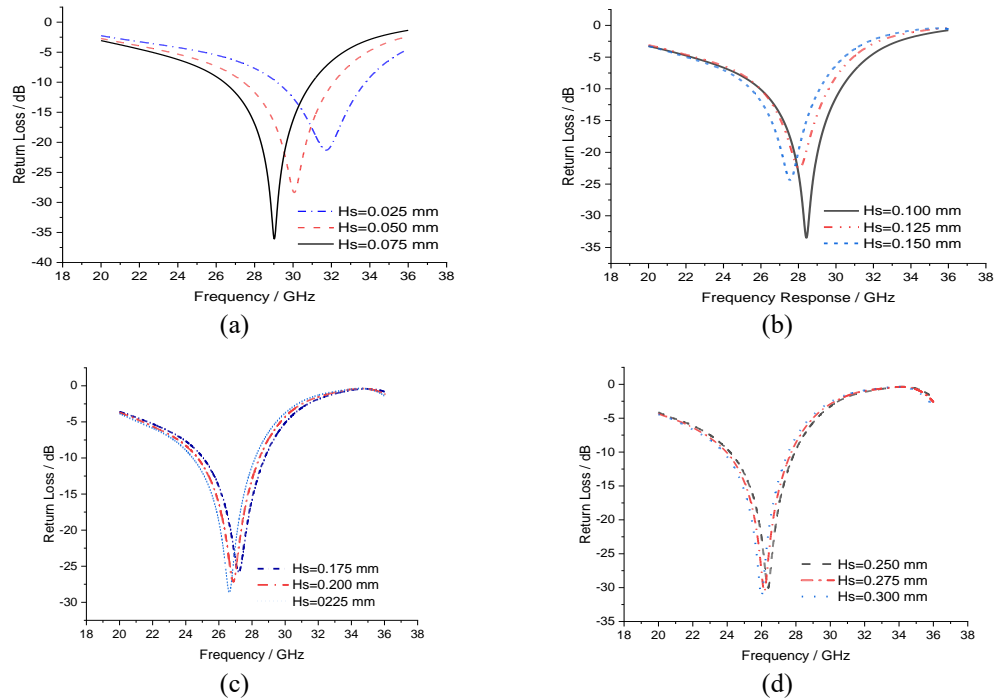

Figure 2. Frequency response characteristics on the following substrate thickness: (a) 0.025 mm to 0.075 mm, (b) 0.100 mm to 0.150 mm, (c) 0.175 mm to 0.225 mm, and (d) 0.250 mm to 0.300 mm

Table 2. Effect of substrate thickness on the antenna parameters

No.	Hs (mm)	Fr (GHz)	Operating bands (GHz)	BW(GHz)	% BW (GHz)	RL (dB)	Gain (dBi)	Dir (dB)	η (%)
1	0.025	31.753	28.541-34.164	5.54	17.45	21.46	3.91	3.98	98.24
2	0.050	30.084	28.541-34.084	5.62	18.68	28.67	3.89	3.97	97.98
3	0.075	29.052	27.44-32.114	4.67	16.07	36.19	3.87	3.97	97.48
4	0.100	28.448	26.477-30.979	4.50	15.82	33.86	3.85	3.97	96.98
5	0.125	28.000	26.200-30.242	4.04	14.43	22.62	3.81	3.96	96.21
6	0.150	27.555	26.004-29.600	3.60	13.06	24.46	3.80	3.96	95.96
7	0.175	27.194	25.462-29.173	3.71	13.64	25.93	3.79	3.97	95.47
8	0.200	26.867	25.14-28.777	3.64	13.55	27.18	3.79	3.97	95.47
9	0.225	26.600	24.587-28.164	3.58	13.46	28.74	3.80	3.98	95.48
10	0.250	26.391	24.41-28.164	3.75	14.21	30.04	3.79	3.98	95.23
11	0.275	26.172	24.171-27.917	3.75	14.33	30.59	3.80	3.99	95.24
12	0.300	25.999	23.995-27.75	3.76	14.46	31.24	3.80	4.00	95.00
13	0.325	25.844	23.839-27.559	3.72	14.39	32.05	3.80	4.01	94.76
14	0.350	25.705	23.684-27.404	3.72	14.47	32.84	3.81	4.02	94.78
15	0.375	25.585	23.58-27.283	3.70	14.46	33.64	3.82	4.03	94.79
16	0.400	25.481	23.425-27.179	3.75	14.72	35.00	3.81	4.05	94.07
17	0.425	25.360	23.079-27.024	3.95	15.58	35.30	3.83	4.06	94.33
18	0.450	25.261	22.975-26.851	3.88	15.36	35.59	3.84	4.08	94.12
19	0.475	25.204	22.906-26.747	3.84	15.24	36.19	3.85	4.09	94.13
20	0.500	25.135	22.837-26.644	3.81	15.16	35.74	3.85	4.11	93.67
21	0.525	25.026	22.711-26.577	3.87	15.46	36.22	3.89	4.13	94.19
22	0.550	24.995	22.672-26.595	3.92	15.68	36.65	3.91	4.15	94.22
23	0.575	24.904	22.604-26.455	3.85	15.46	36.80	3.93	4.18	94.02
24	0.600	24.857	22.589-26.425	3.84	15.45	35.00	3.93	4.20	93.57
25	0.625	24.823	22.537-26.339	3.80	15.31	31.23	3.95	4.21	93.82
26	0.650	24.772	22.435-26.305	3.87	15.62	30.65	3.97	4.24	93.63
27	0.675	24.721	22.384-26.288	3.90	15.78	30.75	4.01	4.26	94.13
28	0.700	24.670	22.367-26.237	3.87	15.69	30.35	4.03	4.29	93.94
29	0.725	24.636	22.265-26.169	3.90	15.83	29.27	4.05	4.31	93.97
30	0.750	24.585	22.214-26.135	3.92	15.94	29.42	4.08	4.34	94.01

The antenna achieved a peak gain of 3.81 dBi, a BW of (26.200 GHz - 30.242 GHz), and an average radiation η of 96.21% at the 28 GHz center frequency on the Hs 0.125 mm. The antenna achieved a better BW and radiation η compared with the other related works, as shown in Table 3. The bidirectional radiation pattern enables the antenna for mm-wave applications for wearable devices. These made the antenna be placed in either the front or back position. Table 2 shows the data obtained from the simulation results, which were used to develop the proposed regression models' equations to analyze and evaluate the effect of Hs variation on Fr, G, % BW, RL, and η.

Table 3. Comparison of other work with the proposed design

Ref.	Fr GHz	Sub. type	Sub ε_r	Sub. tan δ	Size (mm^2)	SH (mm)	BW (GHz)	Gain (dBi)	η (%)
[21]	28	FR4	4.40	0.0200	7×7	0.800	2.620	6.59	82.08
[22]	28	PI	3.50	0.0027	5.19×4.73	0.270	1.427	5.33	86.00
[23]	28	Rogers RT6002	2.94	-	6×8	1.520	1.410	3.12	89.25
[24]	28	Rogers RT 4003	3.55	-	12×12	0.240	4.500	4.50	94.00
[25]	28	Polypropylene	2.34	0.0010	-	0.100	0.500	5.14	-
[26]	28	RT Duroid 5880	2.20	0.0040	5×4.4	0.500	0.850	1.00	90.00
This work	28	PI	3.50	0.0027	5×5	0.125	4.710	3.81	96.41

3.2. Fabrication result and discussion

A sputtering machine deposits silver ink on a PI substrate to print the proposed antenna. The one-layer printing process, which used a conductor thickness of one micrometer (1 µm) per round, lacked the required conductivity. Depositing additional layers of paste ink in the printed area has improved the conductivity. The antenna prototype was fabricated and tested to evaluate the validity of the simulated result. The process is cost-effective and safe to use, as the silver ink is toxin-free for the lungs and skin. The printed antenna maintains flexibility without cracking the ink surface, even at the possible maximum bending radius. Figure 3(a) illustrate the proposed antenna prototype, and Figure 3(b) the return loss (reflection coefficient) of S11 parameters, simulated and measured results. Figures 4(a) and (b) illustrate the simulated and measured 2D radiation patterns for the H-plane and E-plane, respectively. The simulated and measured results are in good agreement, confirming their validity. The antenna's radiation η, BW, G, and bidirectional radiation pattern signify its suitability for the proposed mm-wave applications.

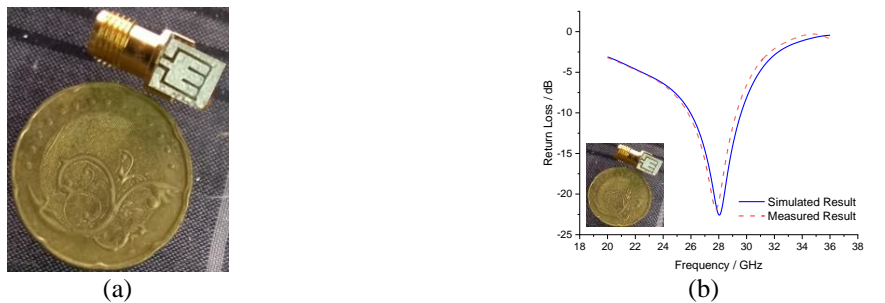(a) (b)

Figure 3. Fabricated antenna and its simulated and measured S$_{11}$: (a) antenna prototype and (b) S$_{11}$ performance
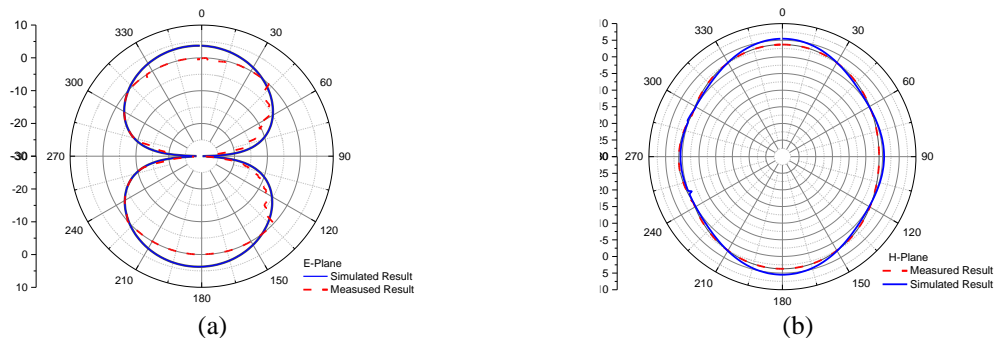

(a) (b)

Figure 4. Simulated and measured 2D radiation patterns: (a) H plane and (b) E plane

3.3. Result analysis

The simulated results have demonstrated the impact of Hs variation on the frequency response characteristics. The average result illustrates how the average values of BW and G increased as the Hs increased and shifted to lower values as the Hs decreased. Generally, the result shows that the higher the Hs, the lower the Fr and η, and the lower the Hs, the higher the Fr and η. These indicate that thinner Hs increase the Fr and radiation η, which improves the antenna's performance. The illustration of a bidirectional radiation pattern enables the antenna to be placed in either the back or front positions. The PI substrate is a polymer-based material that has less power consumption, making the antenna ideal for mm-wave applications in IoT and wearable devices. The measured and simulated S-parameter, E, and H planes are in good agreement. Slightly disturbed due to conductor and dielectric effects, causing impedance mismatches that slightly affected the fabricated results, but they are still in good correlation. Future work needs to investigate the impact of Hs variation on the radiation patterns and impedance matching on the microstrip antenna's performance.

3.4. Comparative analysis

The proposed antenna achieved a wider BW and higher radiation η compared with the other related articles reported in the literature, as shown in the summary in comparison Table 3. The improvement is primarily attributed to the selection of a suitable thin Hs, which enhanced both radiation η and BW. This has made the microstrip antenna suitable for the proposed mm-wave applications. The measured and simulated results in this research work are correlated, confirming the validity of the results.

4.   DEVELOPMENT OF MATHEMATICAL MODEL
4.1. Model design

The data (simulation result) was used to develop the proposed model equations using the MINITAB software. The Hs is the predictor variable, while the Fr, G, % BW, RL, and η are the response variables. Many models were developed in linear, quadratic, and cubic forms and analyzed, evaluated, and validated. The model with the least residual value on the fitted line plots and residual plots indicates the model's fitness to the data and is considered the proposed regression model. And the model is validated by checking the significance of the model coefficients, *R-Sq* and *R-Sq(adj)*, and testing the hypotheses' P-value. The *R-Sq* and *R-Sq(adj)* values closer to 1 and the P-value less than the significance level α (0.05) indicate the model validity. The proposed models are to investigate the impact of the predictor variable (Hs) on the response variables (Fr, G, BW, RL, and η). Figure 5 illustrates the flow chart of the model design procedures.

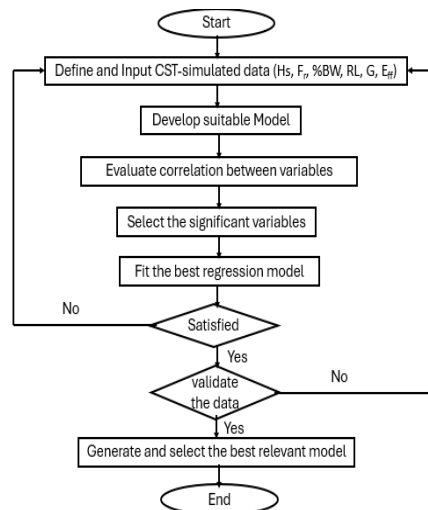
Figure 5. Flow chart

4.2. Model testing

The proposed regression models were tested for their validity and acceptability. Hypotheses (P-value) and *R-Sq* were tested to determine the fitness and validity of the models. The *R-sq* value is between 0 and 1; the *R-sq* value that is closer to 1, and the P-value is less than 0.05, indicating the model's fitness and validity [27]. The developed models achieved the following results: *R-sq* values are 94.6%, 72.1%, 97.9%, 41.5%, and 96.1% for the Fr, % BW, G, RL, and η, respectively. These results indicate the validity of the models except the RL

model, whose value is closer to zero, 41% (0.41), which indicates insufficient evidence to conclude the model's validity. Still, the RL model P-value is 0.00, indicating the model's fitness and validity. The P-value of all the developed models is less than 0.05, except that of % BW, whose P-value is 0.059, indicating insufficient evidence to validate the model fitness. It does not evaluate the overall model's fitness. Thus, the % BW *R-Sq* value is 0.72, signifying the model's fitness and acceptability. We can, therefore, conclude that all the proposed models are validated. Table 4 summarizes the models' performance and shows the correlation between the dependent and independent variables. Figures 6(a) to (e) and Figures 7(a) to (e) illustrate the impact of Hs on the fitted line plots; the straight lines indicate the proposed model, while the dotted lines indicate the data (CST-simulated result).

Table 4. The Summary of the model performance

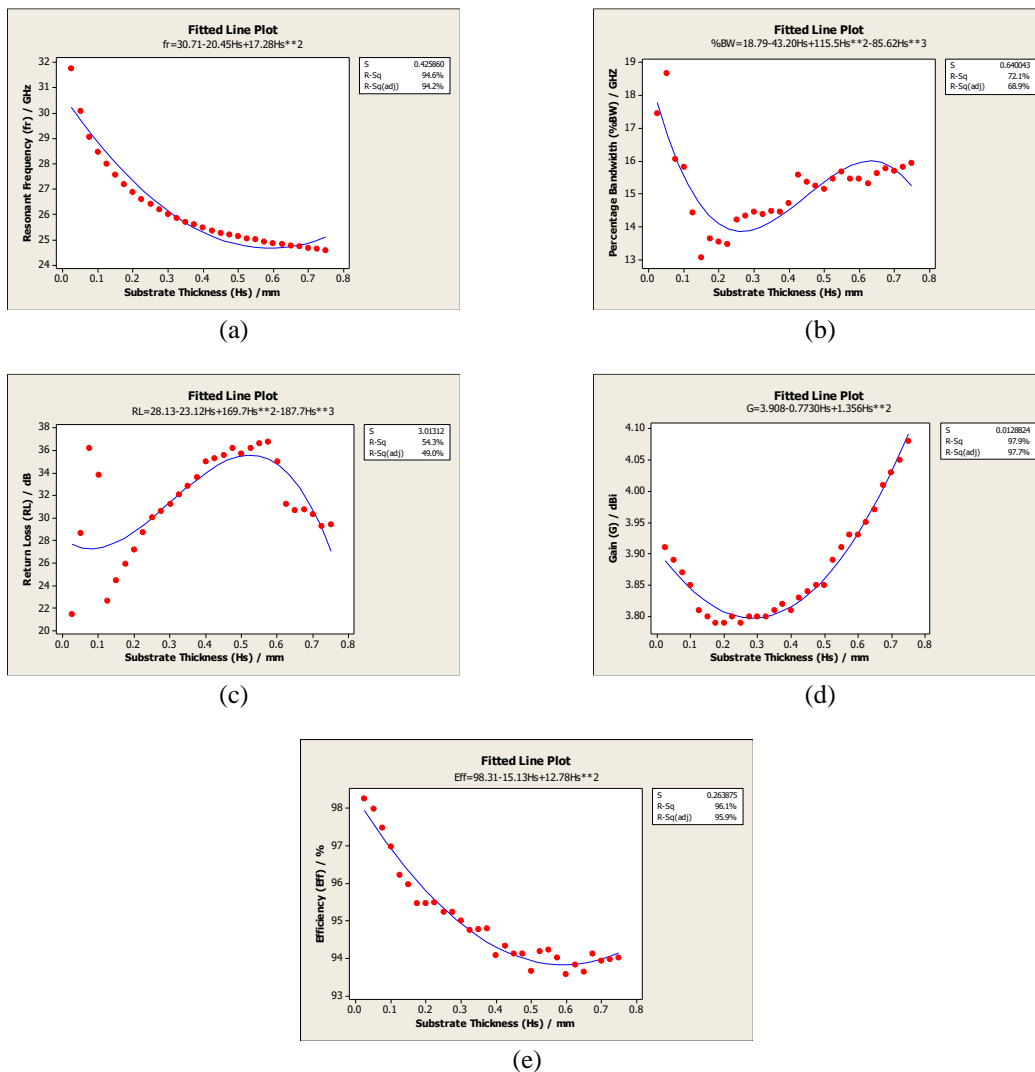| Regression fitness	S	$R-Sq$	$R-Sq(adj)$	r
Center frequency	0.425860	94.6%	94.2%	0.97
Percentage bandwidth	0.640043	72.1%	68.9%	0.85
Gain	0.012882	97.9%	97.7%	0.99
Return loss	3.345330	41.5%	37.1%	0.64
Efficiency	0.263875	96.1%	95.9%	0.98

(a)

(b)

(c)

(d)

(e)

Figure 6. Fitted plot: (a) substrate thickness versus center frequency, (b) substrate thickness versus percentage bandwidth, (c) substrate thickness versus return loss, (d) substrate thickness versus gain, and (e) substrate thickness versus efficiency
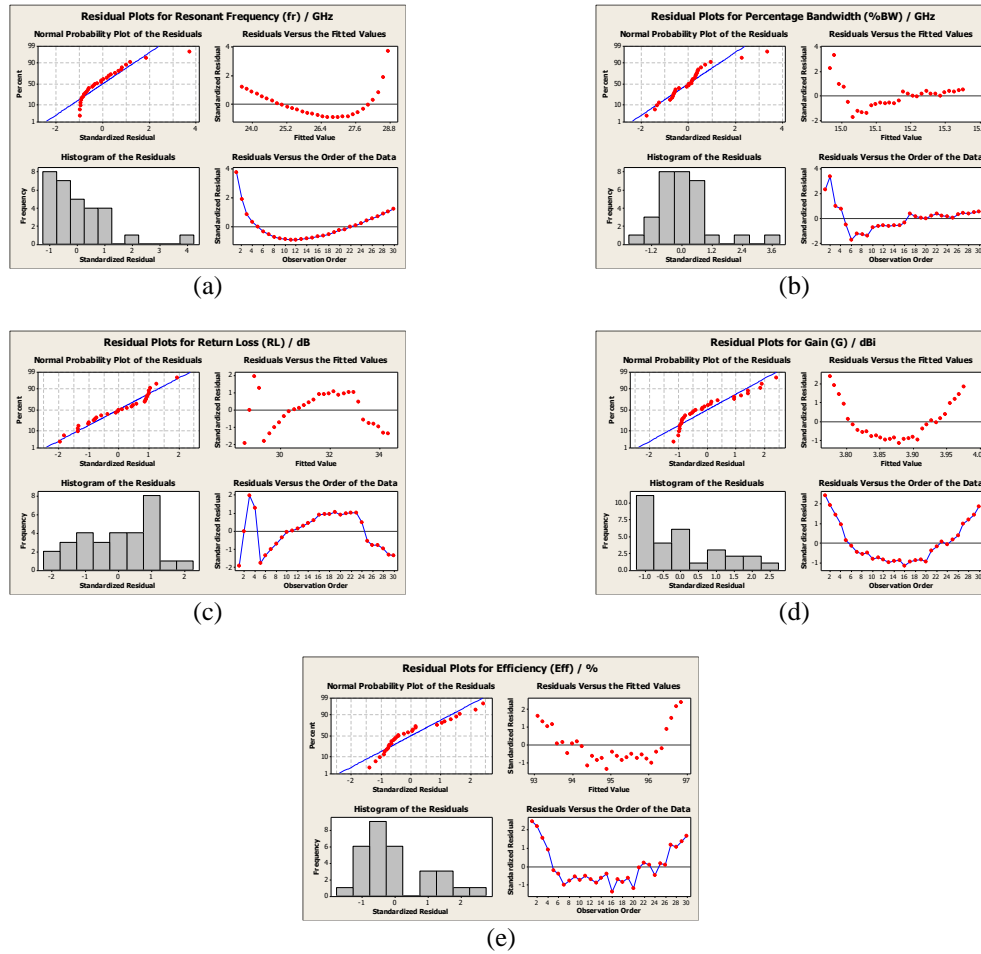
(a)

(b)

(c)

(d)

(e)

Figure 7. Residual plots of four-in-one as a function of fitted values: (a) resonant frequency, (b) percentage bandwidth, (c) return loss, (d) gain, and (e) efficiency

4.3. Developed equation

Analysis of variance (ANOVA) on the developed polynomial regression models and the correlation between the data and the developed regression models. The proposed models' (16), (18), and (20) are quadratic, while (17) and (19) are cubic. The developed regression models were analyzed using the MINITAB software. In the proposed equations, the negative coefficients on the Hs indicate that the average responses of the antenna parameters (Fr, G, % BW, RL, and η) increase as the Hs decreases, and the positive coefficient indicates a decrease in the response variable as the Hs increases. The proposed equations can provide accurate information for a fast solution to filtering the design parameters. To avoid the computational cost and produce a low-profile antenna.

$$Resonant\ Frequency\ (GHz) = 30.71 - 20.45Hs + 17.28Hs^2 \tag{16}$$

$$Percentage\ bandwidth\ (GHz) = 18.79 - 43.20Hs + 115.5Hs^2 - 85.62Hs^3 \tag{17}$$

$$Gain(dBi) = 32.908 - 0.7730Hs + 1.356Hs^2 \tag{18}$$

$$Return\ loss(dB) = 28.13 - 23.12Hs + 169.7Hs^2 - 187.7Hs^3 \tag{19}$$

$$Efficiency(\%) = 98.31 - 15.13Hs + 12.78Hs^2 \tag{20}$$

4.4. ANOVA on the fitness of the developed model

The ANOVA table determines the performance of the developed models, evaluates and validates the results, and determines the significance of the models. To assess the models' fitness to the data provided and to validate the fitted line and residual plots of the models. Tables 5 and 6 present the ANOVA results for the model

fitness and acceptability. When the P-value is <0.05, the null hypothesis (H0) is rejected, signifying that the model fits the data; for the P-value >0.05, the H0 is accepted, meaning that the model does not fit the data [27].

Table 5. ANOVA on the model fitness

Predictor versus response variables	Source	Regression	Residual error	Total
Resonant frequency versus substrate thickness	DF	1	28	29
	SS	70.116	20.548	90.664
	MS	70.116	0.734	
	F	95.54		
	p	0.000		
Percentage bandwidth versus substrate thickness	DF	3	26	29
	SS	27.5305	10.6510	38.1815
	MS	9.17684	0.40965	
	F	22.40		
	P-value	0.000		
Return loss versus substrate thickness	DF	2	27	29
	SS	214.092	302.163	516.256
	MS	107.046	107.046	
	F	9.57		
	P-value	0.001		
Gain versus substrate thickness	DF	2	27	29
	SS	0.204666	0.004481	0.209147
	MS	0.102333	0.000166	
	F	616.62		
	P-value	0.000		
Efficiency versus substrate thickness	DF	2	27	29
	SS	46.9208	1.8800	48.8008
	MS	23.4604	0.0696	
	F	336.93		
	P-value	0.000		

Table 6. Sequential ANOVA

Predictor versus response variables	Source	Linear	Quadratic	Cubic
Resonant frequency versus substrate thickness	DF	1	1	
	SS	70.1159	15.6513	
	F	95.54		
	p	0.000	0.000	
Percentage bandwidth versus substrate thickness	DF	1	1	1
	SS	0.4002	13.3687	13.7616
	F	0.30	14.79	33.59
	P-value	0.590	0.001	0.000
Return loss versus substrate thickness	DF	1	1	1
	SS	90.804	123.288	66.111
	F	5.98	11.02	7.28
	P-value	0.021	0.003	0.012
Gain versus substrate thickness	DF	1	1	
	SS	0.108280	0.096386	
	F	30.06	580.79	
	P-value	0.000	0.000	
Efficiency versus substrate thickness	DF	1	1	
	SS	38.3528	8.5680	
	F	102.78	123.05	
	P-value	0.000	0.000	

4.5. ANOVA on the sequential prediction

Table 7 shows ANOVA on sequential prediction; Hs predicts the response variables (Fr, BW, G, RL, and η). In the ANOVA table, T-values represent the standard errors of the regression coefficient, and a high T-value with the least P-value indicates that the model is of substantial significance. The Coef (coefficient) shows the direction and size of the relationship between the predictor and response variables. A positive Coef indicates a positive relationship, while a negative Coef indicates a negative relationship between the variables. This signifies that the negative Coef in Hs-values on the Fr and η relationship indicates a continuous decrease in the Fr and η values as Hs-values increase. SE Coeff represents the standard error of the Coef; the higher SE Coef indicates less confidence in the predicted values, while the smaller SE Coef signifies a more precise prediction. A P-value less than the significance level (0.05) indicates a significant relationship between the predictor and response variable, and a P-value greater than the significance level of 0.05 indicates an insignificant

relationship between the variables. To confirm the model's precision and validity. The P-values of 0.000 and 0.021 signify the model's significance and acceptability, while the P-value of 0.059 indicates poor model fitness. A P-value greater than 0.05 indicates insufficient evidence to validate the model fitness and acceptability; it does not evaluate the overall model fitness and acceptability. The 4-in-one residual plots can further assess the regression model's fitness and acceptability.

Table 7. Sequential prediction ANOVA

Predictor versus response variables	Predictor	Constant	Hs
Resonant frequency versus substrate thickness	Coef	28.9270	-7.0651
	SE Coef	0.3208	0.7228
	T-value	90.17	-9.77
	P-value	0.000	0.000
Percentage bandwidth versus substrate thickness	Coef	14.9518	0.5337
	SE Coef	0.4350	0.9801
	T-value	34.37	0.54
	P-value	0.000	0.590
Return loss versus substrate thickness	Coef	28.340	8.040
	SE Coef	1.460	3.289
	T-value	19.41	2.44
	P-value	0.000	0.021
Gain versus substrate thickness	Coef	3.76775	0.27764
	SE Coef	0.02248	0.05064
	T-value	167.64	5.48
	P-value	0.000	0.000
Efficiency versus substrate thickness	Coef	96.9878	-5.2253
	SE Coef	0.2287	0.5154
	T-value	423.99	-10.14
	P-value	0.000	0.000

4.6. Residual plot

The residual plots include residual value versus data order, in which the mean values are zero (0) for the model to be valid. Figures 7(a) to (e) include a histogram of the residuals, which indicates the distribution of errors to assess whether the model is appropriate for the data, confirm the model's fitness, and its acceptability. The model errors are more on -1, 0, 1, -1, and -0.5 as shown in Figures 7 (a) to (e), respectively. These fall within the model error limit close to the trend line to signify the model's fitness and validity. The histogram residuals confirm the normality assumptions, as the mean values are approximately zero and the data points are within ±2 standard errors, which corresponds to a 95% confidence interval. The standardized residuals, calculated from the regression standard errors, must be within the range of ±2, which is approximately 95% of the data points [28].

5. CONCLUSION

This research work simulated and fabricated a 28 GHz microstrip antenna and developed and proposed regression model equations to investigate and evaluate the impact of Hs variation on Fr, G, % BW, RL, and η. The fitted line plots analyzed the correlation between the data and the developed models. The antenna was printed on a flexible PI substrate using silver ink to avoid computational cost and fast solutions for filtering design parameters, which is the main objective of the proposed design. The models' equations and experimental results were validated. This was done by comparing the simulated and measured results and the ANOVA of the model characteristics. The measurement shows good agreement with the simulation results. The lower Hs achieved an improved BW and η, a low-cost and low-profile antenna for future mm-valve applications. The model equations can accurately and faster predict the antenna's parameters (Fr, BW, G, RL, and η) and overall antenna performance than many commercially available advanced simulation tools. This gives an insight into how antenna designers can predict the antenna's parameters and performance. These methods could reduce the cost of production and improve the antenna's optimum performance. This paper suggested that the regression models can be expanded to evaluate additional antenna parameters, such as radiation patterns and polarization, to enhance the antenna performance. It also meant the proposed design should be used in frequency-sensitive applications. This article is the first to use the polynomial regression model equations to evaluate the impact of Hs variation on the 28 GHz printable microstrip antenna to the best of our knowledge. The paper suggested extending the proposed regression modeling approach to evaluate additional parameters such as radiation patterns, polarization, and impedance-matching characteristics. It also suggested regression modeling to evaluate the impact of Hs on various parameters in the Terahertz frequencies. Moreover, it suggested that future

advancements in microstrip antenna technology should focus on modern integration techniques to optimize the overall antenna performance for future applications.

AUTHOR CONTRIBUTIONS STATEMENT

This journal uses the Contributor Roles Taxonomy (CRediT) to recognize individual author contributions, reduce authorship disputes, and facilitate collaboration.

Name of Author	C	M	So	Va	Fo	I	R	D	O	E	Vi	Su	P	Fu
Bello Abdullahi Muhammad	✓	✓	✓	✓	✓	✓		✓	✓	✓	✓			
Mohd Fadzil Ain	✓	✓		✓	✓	✓	✓	✓		✓	✓	✓	✓	✓
Mohd Nazri Mahmud	✓				✓	✓				✓	✓	✓		
Mohd Zamir Pakhuruddin	✓	✓		✓	✓	✓	✓			✓	✓	✓		
Ahmadu Girgiri	✓	✓		✓	✓	✓				✓	✓			
Mohamad Faiz Mahamed Omar	✓	✓		✓	✓	✓				✓				

C : **C**onceptualization	I : **I**nvestigation	Vi : **Vi**sualization
M : **M**ethodology	R : **R**esources	Su : **Su**pervision
So : **So**ftware	D : **D**ata Curation	P : **P**roject administration
Va : **Va**lidation	O : Writing - **O**riginal Draft	Fu : **Fu**nding acquisition
Fo : **Fo**rmal analysis	E : Writing - Review & **E**diting	

CONFLICT OF INTEREST STATEMENT

Authors state no conflict of interest.

DATA AVAILABILITY

The data that support the findings of this study are available from the corresponding author, [Mohd Fadzil Ain], upon reasonable request.

REFERENCES

[1] A. Ahmed *et al.*, "Toroidal dipole metasurface based on polyimide substrate for flexible electronic applications," *IEEE Antennas and Wireless Propagation Letters*, vol. 23, no. 7, pp. 2081–2085, Jul. 2024, doi: 10.1109/LAWP.2024.3381255.

[2] R. Singh, B. S. Dhaliwal, and G. Saini, "Design and performance analysis of a Polyimide film substrate-based flexible microstrip antenna with different thicknesses for 2.45 GHz ISM band applications," in *2024 5th International Conference on Recent Trends in Computer Science and Technology (ICRTCST)*, Apr. 2024, pp. 371–375. doi: 10.1109/ICRTCST61793.2024.10578404.

[3] B. G. P. Shariff, S. Pathan, P. R. Mane, and T. Ali, "Characteristic mode analysis based highly flexible antenna for millimeter wave wireless applications," *Journal of Infrared, Millimeter, and Terahertz Waves*, vol. 45, no. 1–2, pp. 1–26, Feb. 2024, doi: 10.1007/s10762-023-00957-8.

[4] S. Alamdar, S. Bagherkhani, F. De Flaviis, and S. Saadat, "Millimeter wave dual-band antenna array on a thin flexible substrate for 5G applications," in *2024 United States National Committee of URSI National Radio Science Meeting (USNC-URSI NRSM)*, Jan. 2024, pp. 61–62. doi: 10.23919/USNC-URSINRSM60317.2024.10464834.

[5] S. Qureshi, M. Hanif, V. Jeoti, G. M. Stojanović, and M. T. Khan, "Review of fabrication of SAW sensors on flexible substrates:

Challenges and future," *Results in Engineering*, vol. 22, Jun. 2024, doi: 10.1016/j.rineng.2024.102323.

[6] M. S. Ali, J. Rains, J. Kazim, F. A. Tahir, M. Imran, and Q. H. Abbasi, "PET based flexible intelligent reflective surface for millimeter-wave applications," in *2024 IEEE International Symposium on Antennas and Propagation and INC/USNC-URSI Radio Science Meeting (AP-S/INC-USNC-URSI)*, Jul. 2024, pp. 1971–1972. doi: 10.1109/AP-S/INC-USNC-URSI52054.2024.10686363.

[7] S. Ermış, "The effect of substrate dielectric constant and thickness on millimeter wave band patch antenna performance," *Celal Bayar Üniversitesi Fen Bilimleri Dergisi*, vol. 20, no. 4, pp. 40–59, Dec. 2024, doi: 10.18466/cbayarfbe.1514216.

[8] D. Ziani, M. Belkheir, M. Rouissat, and A. Mokaddem, "Design optimization for improving the performance of rectangular antennas using polyimide (PI) and liquid crystal (LC) polymers substrates," *Polymer Bulletin*, vol. 81, no. 9, pp. 8447–8469, Jun. 2024, doi: 10.1007/s00289-023-05114-8.

[9] S. Saleh, T. Saeidi, N. Timmons, and F. Razzaz, "A comprehensive review of recent methods for compactness and performance enhancement in 5G and 6G wearable antennas," *Alexandria Engineering Journal*, vol. 95, pp. 132–163, May 2024, doi: 10.1016/j.aej.2024.03.097.

[10] Z. Peng, A. Ye, L. Zhang, X. Li, C. Lian, and C. Li, "Micro-crosslinked polyimide nanocomposites with low dielectric constant and low dielectric loss for microwave antenna with molecular dynamics," *Composites Communications*, vol. 46, Feb. 2024, doi: 10.1016/j.coco.2023.101804.

[11] T. H. Le *et al.*, "Wideband antennas on thin-film packaging substrates for 140 GHz 6G applications," in *2024 IEEE 74th Electronic Components and Technology Conference (ECTC)*, May 2024, pp. 732–737. doi: 10.1109/ECTC51529.2024.00119.

[12] J. Colaco and R. B. Lohani, "Performance analysis of microstrip patch antenna using a four-layered substrate of different materials," *Materials Today: Proceedings*, vol. 52, pp. 1891–1900, 2022, doi: 10.1016/j.matpr.2021.11.522.

[13] B. Luo, X. Liang, H. Chen, N. Sun, H. Lin, and N. Sun, "Gain enhancement and ground plane immunity of mechanically driven thin-film bulk acoustic resonator magnetoelectric antenna arrays," *Advanced Functional Materials*, vol. 34, no. 39, Sep. 2024, doi: 10.1002/adfm.202403244.

[14] B. Sindhu, V. Adepu, P. Sahatiya, and S. Nandi, "An MXene based flexible patch antenna for pressure and level sensing applications," *FlatChem*, vol. 33, May 2022, doi: 10.1016/j.flatc.2022.100367.

[15] R.-Z. Tang, S.-W. Qu, and S. Yang, "Lightweight broadband phased array antenna based on ultra-thin polyimide film," *IEEE Antennas and Wireless Propagation Letters*, vol. 23, no. 7, pp. 2244–2248, Jul. 2024, doi: 10.1109/LAWP.2024.3386776.

[16] P. Lukacs, A. Pietrikova, I. Vehec, and P. Provazek, "Influence of various technologies on the quality of ultra-wideband antenna on a polymeric substrate," *Polymers*, vol. 14, no. 3, Jan. 2022, doi: 10.3390/polym14030507.

[17] G. James, D. Witten, T. Hastie, R. Tibshirani, and J. Taylor, "Linear regression," in *An introduction to statistical learning: with applications in python*, 2023, pp. 69–134. doi: 10.1007/978-3-031-38747-0_3.

[18] F. Tahmasebinia, R. Jiang, S. Sepasgozar, J. Wei, Y. Ding, and H. Ma, "Implementation of BIM energy analysis and Monte Carlo simulation for estimating building energy performance based on regression approach: A case study," *Buildings*, vol. 12, no. 4, Apr. 2022, doi: 10.3390/buildings12040449.

[19] M. Hammouda, M. Ghienne, J.-L. Dion, and N. Ben Yahia, "Linear regression and artificial neural network models for predicting abrasive water jet marble drilling quality," *Advances in Mechanical Engineering*, vol. 14, no. 9, Sep. 2022, doi: 10.1177/16878132221123426.

[20] A. S. Ashoor, A. A. K. Kazem, and S. Gore, "An interactive network security for evaluating linear regression models in cancer mortality analysis and self-correlation of errors by using Durbin-Watson tests in Babylon/Iraq," *Journal of Physics: Conference Series*, vol. 1804, no. 1, Feb. 2021, doi: 10.1088/1742-6596/1804/1/012127.

[21] B. A. Nia, F. De Flaviis, and S. Saadat, "Flexible quasi-yagi-uda antenna for 5G communication," in *2021 IEEE International Symposium on Antennas and Propagation and USNC-URSI Radio Science Meeting (APS/URSI)*, Dec. 2021, pp. 115–116. doi: 10.1109/APS/URSI47566.2021.9704275.

[22] W. A. Awan, S. I. Naqvi, A. H. Naqvi, S. M. Abbas, A. Zaidi, and N. Hussain, "Design and characterization of wideband printed antenna based on DGS for 28 GHz 5G applications," *Journal of Electromagnetic Engineering and Science*, vol. 21, no. 3, pp. 177–183, Jul. 2021, doi: 10.26866/jees.2021.3.r.24.

[23] H. M. A. Rahman, M. N. A. Shovon, M. M. Khan, and T. M. Alanazi, "Dual-band self-complementary 5G antenna for wireless body area network," *Wireless Communications and Mobile Computing*, vol. 2023, pp. 1–18, Apr. 2023, doi: 10.1155/2023/6513526.

[24] A. R. Sabek, A. A. Ibrahim, and W. A. Ali, "Dual-band millimeter wave microstrip patch antenna with stubresonators for 28/38 GHz applications," *Journal of Physics: Conference Series*, vol. 2128, no. 1, Dec. 2021, doi: 10.1088/1742-6596/2128/1/012006.

[25] K. Hu, Y. Zhou, S. K. Sitaraman, and M. M. Tentzeris, "Fully additively manufactured flexible dual-band slotted patch antenna for 5G/mmwave wearable applications," in *2022 IEEE International Symposium on Antennas and Propagation and USNC-URSI Radio Science Meeting (AP-S/URSI)*, Jul. 2022, pp. 878–879. doi: 10.1109/AP-S/USNC-URSI47032.2022.9886082.

[26] V. Sharma, N. K. Mishra, A. Agarwal, and N. L. Gupta, "Small size broadband printed antenna for 5G applications covering 28 GHz/38 GHz and 60 GHz bands," *Gazi University Journal of Science*, vol. 37, no. 1, pp. 211–220, Mar. 2024, doi: 10.35378/gujs.1178594.

[27] I. N. Illa, T. C. Sin, R. Fadzli, I. Safwati, A. Rosmaini, and M. Fathullah, "Product defect prediction model in food manufacturing production line using multiple regression analysis (MLR)," in *AIP Conference Proceedings*, 2021. doi: 10.1063/5.0052688.

[28] T. T. Stanislas *et al.*, "Multivariate regression approaches to predict the flexural performance of cellulose fibre reinforced extruded earth bricks for sustainable buildings," *Cleaner Materials*, vol. 7, Mar. 2023, doi: 10.1016/j.clema.2023.100180.

BIOGRAPHIES OF AUTHORS

Bello Abdullahi Muhammad 🔟 🔠 🆂🅲 🅲 received his B.Eng. degree in Electrical and Electronic Engineering from Kwara State University Nigeria, an M.Sc. degree in Electrical and Electronic Engineering from Coventry University United Kingdom (UK), in 2015, and he is currently pursuing a Ph.D. degree in Antenna and Wave Propagation at the School of Electrical and Electronic Engineering, Universiti Sains Malaysia, His current research interests include communication signal processing, printable antenna, multiband antenna, and millimeter-wave antenna. He has been a lecturer at the Department of Electrical and Electronic Engineering, Abdu Gusau Polytechnic, Talata Mafara, Nigeria. He can be contacted at email: engr.mbabdullahi@student.usm.my.

Mohd Fadzil Ain received BS degree in Electronic Engineering from Universiti Technologi Malaysia, Malaysia (UTM) 1997, M.S. in Radiofrequency and Microwave from Universiti Sains Malaysia (USM) Malaysia in 1999, Ph.D. degree in Radio Frequency and Microwave from the University of Birmingham, United Kingdom in 2003. In 2003 he joined the School of Electrical and Electronics Engineering, he is currently a Professor, a former Dean of the School of Electrical and Electronic, and the Director of Collaborative Microelectronic Design Excellence Centre (CEDEC), USM. He is actively involved in technical consultancy with several companies in microwaves equipment. His research interests include MIMO wireless systems, FPGA/DSP, Ka-band transceiver design, dielectric antenna, and RF characteristics of dielectric material. He is awards and honors include the International Invention Innovation Design and Technology Exhibition, International Exposition of Research and Inventions of Institutions of Higher Learning, Malaysia Technology Expo, Malaysia, and many more. He can be contacted at email: eemfadzil@usm.my.

Mohd Nazri Mahmud received a B.Eng. degree in Electronic Systems Engineering (Telecommunications) from the Department of Electronic Systems Engineering, University of Essex, United Kingdom, in 1996, and an M.Phil. degree in Technology Policy and a Ph.D. degree in Engineering both from the University of Cambridge, United Kingdom, in 2003 and 2022, respectively. He has been a lecturer at the School of Electrical and Electronic Engineering, Universiti Sains Malaysia, since 2006. Previously, he was with Telekom Malaysia from 1996 to 2006. He can be contacted at email: nazriee@usm.my.

Mohd Zamir Pakhuruddin received a B.Eng. in Electrical Engineering from the University of Sheffield, United Kingdom. He spent about 8 years as a Senior Photolithography and Sputtering (R&D) Engineer at SilTerra and Fuji Electric, Kulim Hi-Tech Park, respectively. In 2012, he graduated with an M.Sc. in Physics at Universiti Sains Malaysia (USM), where he researched silicon thin-film solar cells on flexible substrates. In 2016, he obtained his Ph.D. in Photovoltaic Engineering from the University of New South Wales (UNSW), Australia, where he worked on the development of light-trapping schemes in e-beam evaporated laser-crystallized silicon thin-film solar cells on glass superstrates. He is currently an Associate Professor, he is a Director at the Institute of Nano Optoelectronics Research and Technology (INOR) and a Lecturer at the School of Physics, Universiti Sains Malaysia. His research includes black silicon, perovskite, organic, thin-film solar cells for conventional solar windows, optoelectronic devices, and indoor photovoltaic applications. He can be contacted at email: zamir@usm.my.

Ahmadu Girgiri received a B.Eng. degree in Electrical Engineering from Bayero University Kano, Nigeria, in 2008 and an M.Sc. in Information and Communication Technology from the University of Wolverhampton, United Kingdom, in 2013. He is working toward a Ph.D. in Antenna and Propagation at the School of Electrical and Electronic Engineering, Universiti Sains Malaysia, Malaysia. He works with the Department of Electrical and Electronic Engineering, Mai Idris Alooma Polytechnic, Geidam, Yobe-Nigeria. He is a communication and wireless services consultant at Array Digital and Communications, Kano, Nigeria. His research interests include RF and mobile communication, wireless sensor systems, and on-chip design for sub-6 GHz and 5G. He can be contacted at email: ahmadu.g@student.usm.my.

Mohamad Faiz Mahamed Omar received his B.Eng. degree (Hons.) in Electronic Engineering and an M.Sc. degree in RF Microwave Engineering from USM, Nibong Tebal, in June 2014 and 2017, respectively. He is currently a research officer at the Collaborative Microelectronic Design Excellence Centre (CEDEC), USM, pursuing a Ph.D. in Electrical Engineering at Universiti Teknologi Malaysia (UTM). His current research interests include the simulation and design of high RF and high-power devices, microwave tomography, and digital image processing. He can be contacted at email: faiz_omar@usm.my.